Experimental Checking

These modes have been experimentally studied using a setup as shown in Fig. 17 at X and Ku bands.

Placing the sample in a waveguide removes the spherical degeneracy, the result being that each mode appears under the form of a set of three lines. However, for a good symmetrical position of the sample in the waveguide two of the three modes can be totally decoupled. For the $n=1$ modes, however, only a single line can never be decoupled.

Figs. 18 and 19 show the results obtained with a sphere 3.9 mm in diameter where $\epsilon=86$ at X and Ku bands. Verification is therefore excellent. These modes lend themselves to interesting applications such as measurement of small dielectric losses in material with a large dielectric constant.[7] The strong concentration of energy given by these modes has allowed us to build a power limiter using the TE_{101} mode of a YIG sphere.[8]

References

[1] P. Debye, "Der Lichtdruck auf Kugeln von behebigem Material," (in German *Ann. Phys.*, vol. 30, ser. 4, pp. 57–136, 1909.
[2] R. D. Richtmyer, "Dielectric resonators," *J. Appl. Phys.*, vol. 10, no. 6, p. 391, June 1939.
[3] J. A. Stratton, *Electromagnetic Theory*. New York: McGraw-Hill, 1941, p. 554.
[4] A. Okaya, "The rutile microwave resonators," *Proc. IRE* (*Correspondence*), vol. 48, p. 1921, November 1960.
[5] A. Okaya and L. F. Barash, "The dielectric microwave resonator," *Proc. IRE*, vol. 50, pp. 2081–2092, October 1962.
[6] H. Y. Yee, "An investigation of microwave dielectric resonators," Microwave Labs., Stanford University, Stanford, Calif., Rept. 1-065, July 1963.
[7] R. O. Bell and G. Rupprecht, "Measurement of small dielectric losses in material with a large dielectric constant at microwave frequencies," *IRE Trans. Microwave Theory and Techniques*, vol. MTT-9, pp. 239–242, May 1961.
[8] L. Courtois, "A new low level limiter for centimeter and millimeter waves," *J. Appl. Phys.*, vol. 38, pp. 1415–1476, March 1967. Also presented at 12th Annual Conf. on Magnetism and Magnetic Materials, Washington, D.C., November 15–18, 1966.

A High-Power UHF Circulator

YOSHIHIRO KONISHI, SENIOR MEMBER, IEEE

Abstract—**The insertion loss, the bandwidth ratio, and the nonlinearity of a high-power UHF circulator are discussed generally with regard to the characteristics, volume, and filling factor of the ferrite. Theory and experiment are made on the high-power circulator with ferrite, where either surface of the ferrite comes into contact with air. A wideband technique in improving the narrowband that is essentially the result of the filling factor of ferrite is also described.**

To avoid the center conductor heating effect, a circulator without a center conductor is described.

Experiments have proven that, for ferrite nonlinearity, the threshold power by spinwave occurs in a polycrystal for CW power even above resonance and is changed by a external field strength, whereas the nonlinearity is not observed in a single crystal.

I. Introduction

THE ORDINARY Y-stripline circulator has been developed and studied by many authors.[1]–[5] However, in the case of a high-power CW circulator important factors for practical use such as temperature rise, ferrite nonlinearity, bandwidth, and insertion loss have not been adequately explained. As an example, nonlinearity occurs in a polycrystal at a comparatively low-power CW even under an above resonance operation, although such a phenomenon is not observed in a single crystal.

First, the general relation between several electrical characteristics of a circulator is studied in Section II. As a result, it becomes clear that the ferrite of the volume necessary for linearity should come into contact with as wide a surface as possible for good heat conductivity. It is also clarified that insertion loss depends only on ηQ values of the ferrite material reaching a minimum value at the optimum external field, and further, that the bandwidth ratio is related to the filling factor of the ferrite.

Second, to satisfy the general requirements already mentioned, analysis is made for the circulator in which either surface of a ferrite plate comes into contact with a small dielectric constant and permeability, such as air, to create a wide surface and volume of ferrite. Wideband techniques to improve the narrowband, essentially caused by the filling factor of the ferrite, are described. For practical use, construction that offsets rising temperature as a result of the center conductor is also considered.

Finally, several experiments confirming both theory and practical use are described.

Manuscript received May 17, 1967; revised August 7, 1967.
The author is with the Technical Research Laboratories, Nippon Hoso Kyokai, Tokyo, Japan.

II. General Considerations

The approximate values of the characteristics of a circulator such as insertion loss L (decibels), bandwidth ratio w, and available maximum power P_{crit}, are obtained by relating the volume τ and the filling factor k_f (=the time average magnetic energy $\bar{W}_m$/time average total magnetic energy $\bar{W}_{mt}$) of the ferrite contained in a symmetrical 3 port under the following assumptions:

First, it is assumed that there exists no magnetic energy inside the ferrite under the same-phase excitation. This assumption is satisfied for the lumped element Y circulator[7]

and is nearly satisfied for a stripline circulator as described in Section III-B.

Second, it is assumed that tensor permeability takes the positive and negative polarized permeability under positive and negative rotational excitation, respectively.

Let ω_3 and ω_2 be the angular eigenfrequencies at which each of the terminals are at open impedance under positive and negative excitations, and let $\tilde{\omega}$ be the eigenfrequency corresponding to rotational excitation when the ferrite is assumed to be an isotropic medium with a permeability of $(\mu_+ + \mu_-)/2 = \tilde{\mu}$.

Since ω_3 and ω_2 are considered to be the perturbed values of $\tilde{\omega}$ caused by perturbation of permeability $\tilde{\mu}$ to $\tilde{\mu}_+$ and $\tilde{\mu}_-$, we get

$$\frac{\omega_2 - \omega_3}{\tilde{\omega}} = \frac{(\mu_+ - \mu_-) \iiint_\tau |H|^2 dv}{2\tilde{\mu} \iiint_V |H|^2 dv} = \frac{\mu_+ - \mu_-}{2\tilde{\mu}} k_f = \eta k_f. \tag{1}$$

The eigenvalues of admittance corresponding to a negative and positive rotational excitation y_2 and y_3 should take $-j(1/\sqrt{3}R)$ and $+j(1/\sqrt{3}R)$ when the reference plane is defined so that the eigenvalue y_1 corresponding to a same-phase excitation is infinite, where R is the characteristic impedance of the junctions. Since y_2 and y_3 are the frequency variations from the center frequency $\tilde{\omega}$ to ω_2 and ω_3, they are connected to the total reactive energy $\tilde{W}_t$ at $\tilde{\omega}$ in the following:[7]

$$\delta y = y_3 = -y_2 = j\frac{2}{3}\delta\omega \cdot \tilde{W}_t = j\frac{\omega_2 - \omega_3}{3}\tilde{W}_t = j\frac{1}{\sqrt{3}R} \qquad \delta\omega = \omega_2 - \tilde{\omega} = \tilde{\omega} - \omega_3 \tag{2}$$

thus

$$(\omega_2 - \omega_3)\tilde{W}_t = \frac{\sqrt{3}}{R}. \tag{3}$$

As the external Q, Q_e takes the value of

$$Q_e = \frac{\tilde{\omega}\tilde{W}_t R}{3}. \tag{4}$$

From (1), (3), and (4)

$$k_f = \frac{2}{\sqrt{3}Q_e}\frac{\tilde{\mu}}{\mu_+ - \mu_-} = \frac{1}{\sqrt{3}Q_e\eta}. \tag{5}$$

Since the voltage at each terminal for the positive rotational excitation with a power of P_{crit} is $1/3\sqrt{RP_{crit}}$, the intensity of an RF magnetic field at the center of the ferrite h_{crit} takes the value of

$$h_{crit} = \tfrac{1}{3}\sqrt{RP_{crit}}h_{max}$$

thus

$$P_{crit} = \frac{9h^2_{crit}}{Rh^2_{max}} \tag{6}$$

where h_{max} is the RF magnetic field intensity for a unit voltage excitation. Considering the relation

$$\frac{1}{2}\tilde{W}_t k_f = \frac{\tilde{\mu}}{2}\iiint_\tau H^* H dv = K\frac{\tilde{\mu}h^2_{max}}{2}\tau \tag{7}$$

where $K=1$ in the case of a uniform field in ferrite, and from (4) through (7), we get

$$P_{crit} = \frac{9h^2_{crit}K\tilde{\omega}(\mu_+ - \mu_-)\tau}{2\sqrt{3}} = kh^2_{crit}(\mu_+ - \mu_-)\tau\omega. \tag{8}$$

Next, the bandwidth ratio w is obtained. The deviation of y_2 and y_3 in amounts of δy_2 and δy_3 corresponding to the deviation of frequency $\delta\omega$ causes the leakage voltage $|S''|$ at the isolated terminal, and is expressed by

$$|S''| = \frac{R}{2}\sqrt{|\delta y_2|^2 + |\delta y_3|^2 - |\delta y_2| \cdot |\delta y_3|}. \tag{9}$$

Substituting into (9) the relation obtained from (2) and (4) and approximating $\delta y_2 \fallingdotseq \delta y^3$ under $c \ll 1$, we get

$$w = 2\sqrt{3}|S''|k_f\eta. \tag{10}$$

Last, the insertion loss L (decibels) is expressed by the magnetic energy for rotational excitations and the corresponding quality factors of $\mu_\pm$, $Q_\pm$, and a quality factor of the dielectric constant of ferrite Q_c as in (11). (See Appendix I.)

$$L = 2.5\frac{1}{\eta}\left(\frac{1}{Q_+} + \frac{1}{Q_-} + \frac{2}{Q_c}\right) \fallingdotseq \frac{5}{\eta}\left(\frac{1}{Q_{eff}} + \frac{1}{Q_c}\right). \tag{11}$$

Equations (8), (10), and (11) show the relation between P_{crit}, w, L and τ, η, Q. Equation (8) shows that a high P_{crit} requires a large volume. It is also understood from (10) that the bandwidth ratio w, which becomes narrower for a smaller filling factor k_f required for a high-power circulator mentioned later and for a smaller η under a stronger dc external magnetic field, is not concerned with the volume τ. From (11) it is also understood that insertion loss L depends only on the $Q\eta$ product of material and not on τ and k_f. Further, an optimum dc magnetic field exists which satisfies the minimum insertion loss under the maximum $Q\eta$ value.

III. Partially Filled Coaxial Y Circulator

Increasing volume τ and surface of the ferrite required for a high-power circulator is possible by making either surface of the ferrite come into contact with an air medium. In this Section the approximate values of eigenvalues are theoretically obtained as a function of the ratio of the width of ferrite to that of an air medium, and to the diameter of the ferrite. Based upon these results, the design considerations for this type of circulator are presented.

A. Analysis

The TM mode exists in a direction perpendicular to the surface of the ferrite where the tangential component of electrical field changes in sinusoidal and exponential variation inside the ferrite and air region, respectively, that is, if the ferrite is assumed to be an isotropic medium.

Using the potential function of the TM mode for a trial function, the eigenfrequencies corresponding to eigenvectors are calculated by the variational technique, and the eigenvalues are obtained by the calculated values of the energies together with corresponding eigenfrequencies.

However, there are variations of (12) corresponding to a trial electric field E, magnetic field H, electric current J, and magnetic current M inside a cavity resonator.

$$\langle EJ^* \rangle_{V+S} + \langle HM^* \rangle_{V+S} = 0 \tag{12}$$

where $\langle\ \rangle$ denotes the sum of the volume integral of scalar product of the continuous region V and the surface integral on discontinuous surface S. The value of ω obtained by solving (12) takes approximate values of the second-order error.[6],[8] Assuming that the ferrite is an isotropic medium with a proper isotropic permeability, we can also obtain the angular frequency ω' by (12) using the same trial function.

However, it has been verified that ω can be obtained by ω' and the perturbational term (13). (See Appendix II.)

$$\omega = \omega' \left\{ 1 - \frac{\iiint_\tau H \cdot (\mathfrak{y}^* - \mu) H^* dv}{2 \iiint_V H \cdot \mathfrak{y}^* H^* dv} \right\}. \tag{13}$$

1) Same-Phase Excitation: The eigenfrequency satisfying the zero impedance at each terminal under a same-phase excitation with unit current is obtained. The trial potential function assumed in (14) corresponds to the first three terms of the infinite series solution and is for air and ferrite, respectively,

$$\begin{aligned} \varphi_1 &= C_1 \cos k_{Z1}(h - Z)\{J_0(k_\rho \rho) + C_3 \cos 3\phi \cdot J_3(k_\rho \rho) \\ &\qquad + C_6 \cos 6\phi \cdot J_6(k_\rho \rho)\}, \\ \varphi_2 &= C_2 \cos k_{Z2} Z\{J_0(k_\rho \rho) + C_3 \cos 3\phi \cdot J_3(k_\rho \rho) \\ &\qquad + C_6 \cos 6\phi \cdot J_6(k_\rho \rho)\} \end{aligned} \tag{14}$$

where

$$C_2 = C_1 \frac{\cos k_{Z1}(h - t)}{\cos k_{Z2} t}$$

from the continuity on the ferrite surface.

Since we have the boundary condition on the periphery of the center conductor

$$\begin{aligned} &E_Z = 0, \quad \phi = \frac{2\pi}{3} m \qquad m = 0, 1, 2, \\ &H_\phi = 0, \quad \frac{\theta}{2} + \frac{2\pi}{3} m < \phi < -\frac{\theta}{2} + \frac{2\pi}{3}(m+1) \\ &\qquad\qquad m = 0, 1, 2 \end{aligned} \tag{15}$$

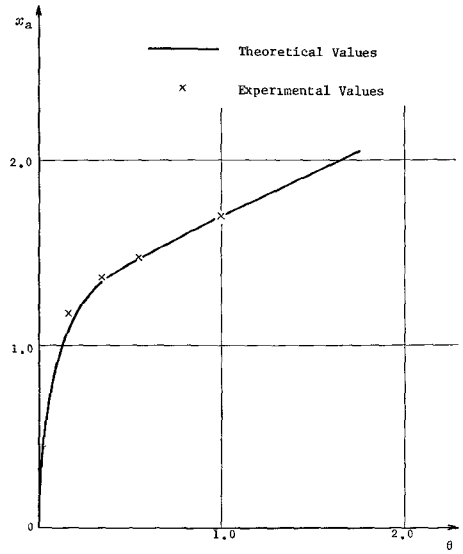

Fig. 1. Values of x_a.

the values of C_3 and C_6 may be selected to satisfy

$$E_Z = 0 \text{ at } \phi = \frac{2\pi}{3} m,$$

and

$$H_\phi = 0 \text{ at } \phi = \frac{2\pi}{6} + \frac{2\pi}{3} m.$$

However, since (14) satisfied Maxwell's equation inside the ferrite and the boundary condition on the broad surface of the ferrite, trial electric currents J_s and the magnetic current M_s may be considered only on the surface $\rho = a$. In this case, J_s flows toward the Z direction to satisfy (15) and M_s flows toward the ϕ direction to connect the mode of (14) with the dominant stripline mode of the feeders. Therefore, substituting the calculated values of J_s and M_s into (12), we get

$$\begin{aligned} &J_0 J_0' + \frac{C_3^2}{2} J_3 J_3' + \frac{C_6^2}{2} J_6 J_6' \\ &-2J_0' \left\{ C_3 \left[\frac{\sin \frac{3}{2}\theta}{\frac{3}{2}\theta} - 1 \right] J_3 + C_6 \left(\frac{\sin 3\theta}{3\theta} - 1 \right) J_6 \right\} = 0 \end{aligned} \tag{16}$$

where

$$J_n = J_n(x_a), \qquad J_n' = J_n'(x_a).$$

The results of calculation of (16) are illustrated in Fig. 1. In the case where $\theta \ll 1$ and where ϕ contains the higher-order terms, x_a may instead be obtained from the infinite series [see (14)] by an approximate integral method which results in

$$J_0(x_a) + 2J_1(x_a) \cdot x_a \cdot C_i\left(\frac{3\theta}{2}\right) = 0. \tag{17}$$

Equation (17) shows that x_a approaches zero as θ approaches zero. However, the values obtained from (16) are almost measurable because θ is larger than 0.5 radian in practical cases.

Next, from the continuity of the surface impedance the following is obtained:

$$\frac{k_{Z1}}{\epsilon_1}\tan k_{Z1}(h-t)+\frac{k_{Z2}}{\epsilon_2}\tan k_{Z2}t=0 \tag{18}$$

and where one can also obtain the relation between wavenumbers

$$\begin{aligned} k\rho^2+k_{Z1}{}^2&=k_1{}^2,\\ k\rho^2+k_{Z2}{}^2&=k_2{}^2 \end{aligned} \tag{19}$$

and

$$k_{Z1}{}^2-k_{Z2}{}^2=k_1{}^2-k_2{}^2 \qquad k_1{}^2=\omega^2\mu_1\epsilon_1,\ k_2{}^2=\omega^2\mu_2\epsilon_2. \tag{20}$$

After obtaining k_{Z1} and k_{Z2} from (18) and (20) and substituting them into (19) using x_a indicated in Fig. 1 we can get ω'. The calculation is further simplified by taking the first two terms of Fourier expansion of the tangent which is sufficient for good approximation in a practical case because

$$\begin{aligned} &k_{Z1}(h-t),\\ &k_{Z2}t<1. \end{aligned} \tag{21}$$

The results are

$$\omega'=\frac{x_a}{a\sqrt{\epsilon_2\mu_{\text{eff}}}}\sqrt{\frac{2\left\{t'+\frac{\epsilon_{2s}}{\epsilon_{1s}}(1-t')\right\}}{\left\{1+\sqrt{1+F^2}\right\}\left\{t'+\frac{\mu_{1s}}{\mu_{\text{eff},s}}(1-t')\right\}}},$$

$$F=\frac{2\sqrt{2}}{\sqrt{3}}\frac{t'(1-t')\left\{t'+\frac{\epsilon_{2s}}{\epsilon_{1s}}(1-t')\right\}^{1/2}}{\left\{t'+\frac{\mu_{1s}}{\mu_{\text{eff},s}}(1-t')\right\}\left\{\frac{\epsilon_{1s}}{\epsilon_{2s}}t'+(1-t')\right\}^{1/2}}\frac{hx_a}{a}$$

$$\epsilon_{1s}=\mu_{1s}=1 \qquad \text{(for air medium)}$$

$$\epsilon_i=\epsilon_0\epsilon_{is},\ \mu_{\text{eff}}=\mu_0\mu_{\text{eff},s}. \tag{22}$$

To obtain the compensating term of (13), we define the vector

$$\boldsymbol{a}^+=\boldsymbol{i}_\rho-j\boldsymbol{i}_\phi, \qquad \boldsymbol{a}^-=\boldsymbol{i}_\rho+j\boldsymbol{i}_\phi \tag{23}$$

and express $\boldsymbol{H}_t=\boldsymbol{i}_\rho H_\rho+\boldsymbol{i}_\phi H_\phi)$ by

$$\boldsymbol{H}_t=a^+\boldsymbol{a}^++a^-\boldsymbol{a}^- \tag{24}$$

where

$$a^+=\frac{H_\rho+jH_\phi}{2}, \qquad a^-=\frac{H_\rho-jH_\phi}{2}$$

$$H_\rho=\frac{1}{\rho}\frac{\partial\varphi}{\partial\phi}, \qquad H_\phi=-\frac{\partial\varphi}{\partial\rho}.$$

where

$$\xi=\frac{2\mu_0}{\mu_++\mu_-}\frac{\cos^2 k_{Z2}t\int_t^h\cos^2 k_{Z1}(h-Z)dZ}{\cos^2 k_{Z1}(h-t)\int_0^t\cos^2 k_{Z2}ZdZ}$$

$$\fallingdotseq\frac{2(1-t')}{t'}\frac{1}{\tilde{\mu}_s} \qquad \tilde{\mu}_s=\frac{\mu_++\mu_-}{2\mu_0}=\frac{\mu_{+s}+\mu_{-s}}{2}.$$

If μ_{eff} is used instead of μ in (13) and (24) is substituted into the second term of (13) we get (25) which is a good approximation in the case where $\eta^2\ll 1$.

$$\frac{\delta\omega}{\omega'}=\frac{\eta\iiint_\tau\{\mu_+|a^+|^2-\mu_-|a^-|^2\}dv}{2\iiint_V\{\mu_+|a^+|^2+\mu_-|a^-|^2\}dv}$$

$$=\frac{\eta^2}{2}\frac{1}{1+\xi} \tag{25}$$

Therefore, (13) can be shown as (26) by using (22) and (25).

$$\omega=\frac{x_a(\theta)}{a\sqrt{\epsilon_2\mu_{\text{eff}}}}\cdot\sqrt{\frac{2\{t'+\epsilon_{2s}(1-t')\}}{\left\{t'+\frac{1}{\mu_{\text{eff},s}}(1-t')\right\}\{1+\sqrt{1+F^2}\}}}\cdot\left\{1-\frac{\eta^2}{2(1+\xi)}\right\}. \tag{26}$$

In an ordinary circulator (26) becomes (27) by substituting $t'=1$

$$\omega=\frac{x_a(\theta)}{a\sqrt{\epsilon_2\mu_{\text{eff}}}}(1-\eta^2). \tag{27}$$

The approximate values of a total reactive energy for the constant unit current same-phase excitation $\tilde{W}_t$ is obtained from a trial function

$$\tilde{W}_t = \frac{6.75}{\omega}\frac{h\lambda}{a^2}\left(\frac{t'}{\epsilon_{2s}} + 1 - t'\right)\frac{I}{J_1^2(xa)} \tag{28}$$

where

$$I = 2\pi\int_0^{x_a} J_0^2(x)xdx + \pi C_3^2\int_0^{x_a} J_3^2(x)\cdot xdx + \pi C_6^2\int_0^{x_a} J_6^2(x)xdx.$$

The energy $\tilde{W}_t'$, as in the case of Fig. 6(b) described later, takes on the values of

$$\tilde{W}_t' = 4\tilde{W}_t. \tag{29}$$

2) Negative and Positive Rotational Excitation: Assuming isotropic permeabilities μ_- and μ_+ by tensor quantity, the potential function adopted for air and ferrite, respectively, is

$$\varphi_1 = C_1' \cos k_{Z1}(h - Z)\cdot e^{\pm j\phi}J_1(k_\rho\rho),$$
$$\varphi_2 = C_2' \cos k_{Z2}Z\cdot e^{\pm j\phi}J_1(k_\rho\rho). \tag{30}$$

From the boundary condition $H_\phi = 0$ at $\rho = a$

$$J_1'(x_a') = 0$$

thus

$$x_a' = k_\rho a = 1.841. \tag{31}$$

The second term of (13) expressed by $a^\pm$ substituting $\mu_\mp$ instead of μ, results in

$$\frac{\delta\omega}{\omega'} = \frac{\pm(\mu_+ - \mu_-)\iiint_\tau |a^\pm|^2 dv}{2\iiint_V \{\mu_+|a^+|^2 + \mu_-|a^-|^2\}dv} \tag{32}$$

where $a^\pm$ can be calculated by (24) and (30). Therefore, the approximate values of $\omega_\mp$ obtained from the above results are

$$\omega_\mp = \frac{1.841}{a\sqrt{\epsilon_2\mu_\mp}}\cdot\sqrt{\frac{2\left\{t' + \frac{\epsilon_{2s}}{\epsilon_{1s}}(1-t')\right\}}{\left\{t' + \frac{\mu_{1s}}{\mu_{\mp s}}(1-t')\right\}\{1+\sqrt{1+F^2}\}}}\cdot\left\{1 \mp \frac{0.063\eta}{0.787\left(1+\frac{1}{\tilde{\mu}_s}\right) \mp 0.66\eta\frac{1-t'}{t'}}\right\}. \tag{33}$$

The total reactive energy $\tilde{W}_{t\mp}'$ is also obtained as

$$\tilde{W}_{t\mp}' \fallingdotseq 0.0725\frac{a^2}{\omega h\lambda\left(1 - t' + \frac{t'}{\epsilon_{2s}}\right)}. \tag{34}$$

The eigenvalues of admittance for negative and positive phase excitations are obtained from (2) as

$$y_\mp = j(\omega - \omega_\mp)\tfrac{2}{3}W_{t\mp}' = j0.0484\frac{a^2}{h\lambda\left(1 - t' + \frac{t'}{\epsilon_{2s}}\right)}\frac{\omega - \omega_\mp}{\omega} \tag{35}$$

where $\omega_\mp$ takes the values of (33).

B. Design Consideration for the Circulator

1) Determination of a Transformer Ratio: A circulator realized by inserting a proper parallel reactance and ideal transformer at each terminal is considered. As the difference of admittance eigenvalues $y_\mp$ should be $y_+ - y = j(2/\sqrt{3}R)$ when the eigenadmittance for a same-phase excitation is infinite, we get from (35)

$$0.0484\frac{a^2}{h\lambda\left(1 - t' + \frac{t'}{\epsilon_{2s}}\right)}\frac{\omega_- - \omega_+}{\omega}n^2 = \frac{2}{\sqrt{3}\,R}. \tag{36}$$

Substituting (33) into $\omega_\mp$ and considering the relation $\mu_\mp \fallingdotseq \tilde{\mu}(1 \mp \eta)$ and the condition $\eta \ll 1$, one obtains

$$n^2 = 1.63\frac{h}{a}\frac{(1 - t' + \tilde{\mu}_s t')^{3/2}\left(1 - t' + \frac{t'}{\epsilon_{2s}}\right)^{1/2}}{t'\eta\tilde{\mu}_s} \tag{37}$$

which is a required transformer ratio.

2) Reactance To Be Inserted at Each Terminal: As discussed in Section III-A, x_a takes different values depending on θ whereas x_a' is independent. Therefore, a capacitive reactance is required under the condition $x_a < x_a'$, which corresponds to $\theta < 1.3$ radians, although no reactance is needed in the case of $x_a = x_a'$.

3) Values of P_{crit}, w, and L: Denote the RF magnetic field at center by h_{crit} for operation with a power P_{crit}

$$h_{crit} = h_\rho = \frac{1}{\rho}\frac{\partial\varphi}{\partial\phi_{\rho=0}} = C_2'\frac{x_a'}{2a}.$$

However, C_2' is obtained from the terminal voltage determined by P_{crit} as

$$C_2' = \frac{n\sqrt{R\,P_{crit}}}{3\omega\mu_+ h\left\{t' + \frac{1}{\mu_{+s}}(1-t')\right\}J_1(x_a')}.$$

Substituting (36) and (26) into n and ω of the preceding equations yields

$$P_{crit} = 0.716 \left\{\frac{1 + (\mu_{+s} - 1)t'}{1 + (\tilde{\mu}_s - 1)t'}\right\}^2 h_{crit}^2 \tau\omega(\mu_+ - \mu_-). \quad (38)$$

4) Bandwidth Ratio w: Equation (9) can also be expressed by the frequency variation of eigenvalues of reflection coefficient as

$$|S''| = \frac{1}{3}\sqrt{\sum_{i=1}^{3} |\delta S_i|^2 - \sum_{i \neq j} |\delta S_i| \cdot |\delta S_j|}. \quad (39)$$

Since we have the relation of $|\delta S_1| = (4/3R)\tilde{W}_{t1}|\delta\omega|$ and $|\delta S_3^2| = (|\delta\omega|/Y)\tilde{W}_{t\mp}'$, substituting (28) into $\tilde{W}_{t1}$ and (34) into $\tilde{W}_{t\mp}$, we get

$$\left|\frac{\delta S_1}{\delta S_i}\right|_{i \neq 1} = 0.087\left(\frac{h\lambda}{a^2}\right)^2 \frac{\left(1 - t' + \frac{t'}{\epsilon_{2s}}\right)^2 I}{J_1^2(x_a)} \ll 1. \quad (40)$$

It is understood that the eigenvalue for the same-phase excitation is very insensitive for a frequency variation other than that of rotational excitation. So, putting $\delta S_1 = 0$ we get

$$w = \frac{2|\delta\omega|}{\omega} = \frac{6|S''|}{n^2\omega\tilde{W}_t R}.$$

If the relation $n^2\omega\tilde{W}_t = \{\omega/(\omega_- = \omega_+)\}(\sqrt{3}/R)$ which is obtained from (34) and (36), is substituted into above equation, we get

$$w = \frac{6|S''|\eta t'\tilde{\mu}_s}{\sqrt{3}\{1 + (\tilde{\mu}_s - 1)t'\}}. \quad (41)$$

On the other hand, the filling factor k_f is calculated from a trial function as

$$k_f = \frac{\tilde{W}_m}{\tilde{W}_{tm}} = \frac{\tilde{\mu}_s t'}{\{1 + (\tilde{\mu}_s - 1)t'\}}. \quad (42)$$

Therefore,

$$w = 2\sqrt{3}|S''|\eta k_f$$

which is the same relation as (10) obtained by general consideration.

5) Insertion Loss: Under the consideration $\tilde{W}_{t1} \ll \tilde{W}_{t\mp}$, the same results can be obtained as in (11).

6) Volume: From the relation $\tau = \pi h t' a^2$ and (26), one obtains

$$\tau \fallingdotseq \frac{x_a^2}{2\pi} h\lambda^2 \frac{\left\{1 - \left(1 - \frac{1}{\epsilon_{2s}}\right)t'\right\} t' \left\{1 - \frac{\eta^2}{2(1+\xi)}\right\}}{\{1 + (\mu_{eff,s} - 1)t'\}\{1 + \sqrt{1 + F^2}\}}. \quad (43)$$

7) Rising Temperature: The heat generated per unit volume is inversely proportional to τ, and the rising temperature T is highest on the boundary surface between air and ferrite and is proportional to the square of the ferrite width if heat escapes only through the surface contacting the metal plate. Therefore we get the relation

$$T \sim \frac{t^2}{\tau} = \frac{t}{a^2} = \frac{ht'}{a^2} \quad (44)$$

which shows T is proportional to a width and inversely proportional to a surface.

8) One Design Procedure: Considering the several conditions previously mentioned one example of design procedure can be shown as follows:

a) μ_{eff}, μ_+, and μ_- are determined to minimize the insertion loss by (11);
b) τ, h, t', and a are determined from P_{crit} of (38) and T of (44) and (26);
c) w is obtained from (41).

C. Consideration of the Wideband

Since the $t' < 1$ required for high power makes the bandwidth narrower from (41), it is preferable to use the wideband technique. However, the frequency variation for same-phase excitation is more insensitive than that of the rotational excitation as shown in (40) and results in the narrow bandwidth. On the other hand, the frequency variations of rotational excitation $\delta S_{2,3}$ are essentially connected to k_f by the following equation derived from (39), (4), and (6):

$$|\delta S_i|_{i \neq 1} = \frac{\delta\omega}{Y}\tilde{W}_{ti} = \frac{\delta\omega}{Y}\frac{3Q_e}{\bar{\omega}R} = \frac{\delta\omega}{\bar{\omega}}\frac{\sqrt{3}}{k_f\eta}.$$

Therefore by increasing reactive energy only for the same phase of excitation it is most effective to make a wideband until satisfying

$$|\delta S_i|_{i \neq 1} = |\delta S_1| = \frac{4}{3R}\tilde{W}_{t1}|\delta\omega| = \frac{|\delta\omega|}{Y}\tilde{W}_{t(i \neq 1)}$$

thus

$$\tilde{W}_{t1} = \frac{3R^2}{4}\tilde{W}_{ti}. \quad (45)$$

One example of the techniques of coupling only to a same-phase excitation is illustrated in Fig. 2(a). The equivalent networks of each excitation are shown in Fig. 2(b) where $L_c'C_c'$ and $L_c''C_c''$ can be neglected in a practical case because their resonant frequencies differ greatly from ω.

Next, the most important factor is the rising temperature on the center conductor; this heats the ferrite surface. This matter could be improved by using the reentrant cavity

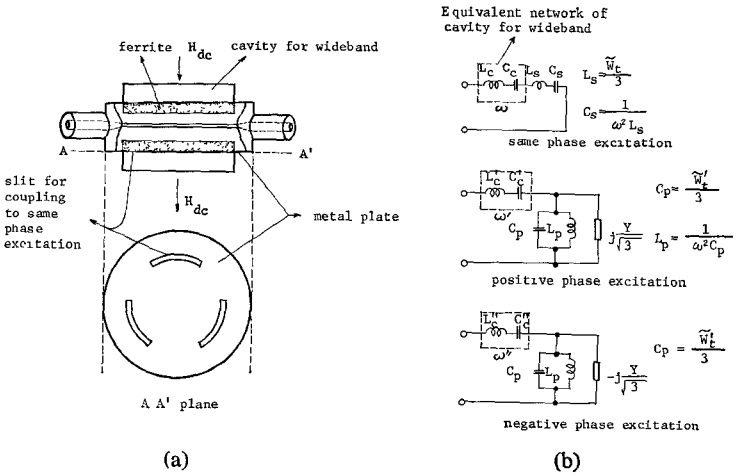

Fig. 2. Wideband technique and the equivalent network. (a) An example of coupling cavity for the wideband to the same-phase excitation. (b) Equivalent network of each eigenvalue. ω: center angular frequency of circulator; $\omega' \neq \omega$; $\omega'' \neq \omega$.

coupled with the coaxial junction as shown in Fig. 6(b) where ferrite is inserted at the narrow space. Since, for the rotational excitation, the TE_{11} mode in the coaxial part inside cavity couples to the quasi TM_{11} mode in ferrite, the length of coaxial part is chosen at a quarter of the TE_{11} mode wavelength. This contributes to an open boundary condition at the periphery of the ferrite disk which is same as an ordinary circulator. For a same-phase excitation, the cavities are nonresonant, and this contributes to maintaining its eigenvalue at a zero impedance which is the same as that of the aforementioned stripline circulator.

IV. Experiments

A. Confirmation of the Theoretical Eigenvalues

The experiment was made with a ferrite disk of 150 mm in diameter, 7 mm in width, where $\epsilon_{2s}=14$ and under the state of $t'=0.425$ and $\theta=0.6$. The measured value of $\mu_{eff,s}$ is 3.2; μ_+ and μ_- are calculated from $\mu_{eff,s}$.

The theoretical values of y_1, y_2, and y_3 calculated from the above data are plotted by a dotted line on Smith chart of Fig. 3; the experimental values are also indicated by lines, which show good coincidence with theoretical values.

B. Nonlinearity of Ferrite

The experiment was made with a lumped element circulator operated at above resonance to use small samples of polycrystals and single crystals of YIG. As indicated in Fig. 4(a), the threshold power P_{crit} occurs at comparably small CW power for polycrystal and it becomes higher for a stronger dc magnetic field. This threshold power was not observed in the single crystal and nonlinearity takes place immediately after power is applied, as the temperature of the ferrite cannot be raised. For pulsed power, the nonlinearity did not appear in the experiment below 2 kW for both polycrystal and single crystal as shown in Fig. 4(b). This phenomenon is supposed to be caused by local heating owing to spinwave generation around pore regions of polycrystals where the internal dc field is below resonance because of the demagnetizing and anisotropic field in their vicinities; and local heating increases in CW power. The increase of P_{crit} for a stronger dc field should be caused by the statistical diminish of the amount of such a grain. From the above reasons, it is preferable to use materials with small values of $\omega_M/\Delta H$, although an excessive value of ΔH of polycrystal should be avoided to keep the insertion loss small.

C. Performance of the Circulator

1) Wideband Characteristics: The characteristics of a trial circulator at 670 MHz with $t'=0.4$ is 25 MHz in bandwidth and 0.2 dB in insertion loss. This becomes wideband, as shown in Fig. 5 by the construction of Fig. 2(a).

2) High-Power Operation: The circulator [Fig. 6(b)] with ferrite of 150 mm in diameter and 5 mm in width was tested by 15 kW CW operation at 670 MHz. The rising temperature of the ferrite surface was 10 degrees higher than the cavity which was cooled by water. The nonlinearity did not occur.

Appendix I

Showing the absolute values of eigenvalues of reflection coefficients S_1, S_2, and S_3 by $e^{-\alpha 1}$, $e^{-\alpha 2}$, and $e^{-\alpha 3}$, and assuming no energy in the same-phase excitation, the insertion loss L (decibels) is

$$L = 8.67 \ln \left(1 - \frac{\alpha_2 + \alpha_3}{3}\right) = \frac{8.67}{3} \sum_{i=2}^{3} \alpha_i. \qquad (46)$$

However,

$$|S_i| = \left|\frac{Y - y_i}{Y + y_i}\right| = 1 - \frac{2Yy_i''}{Y^2 + y_i'^2} \qquad y_i = jy_i' + y_i''.$$

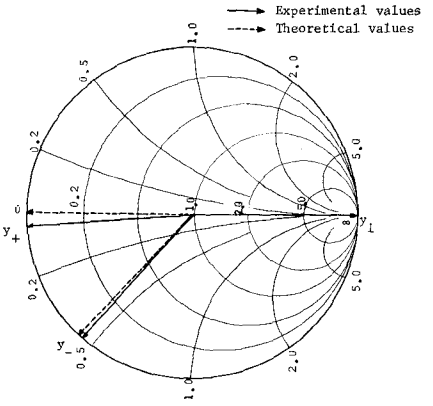

Fig. 3. Comparison of the theoretical values of the eigenvalues with experimental values on the normalized admittance Smith chart.

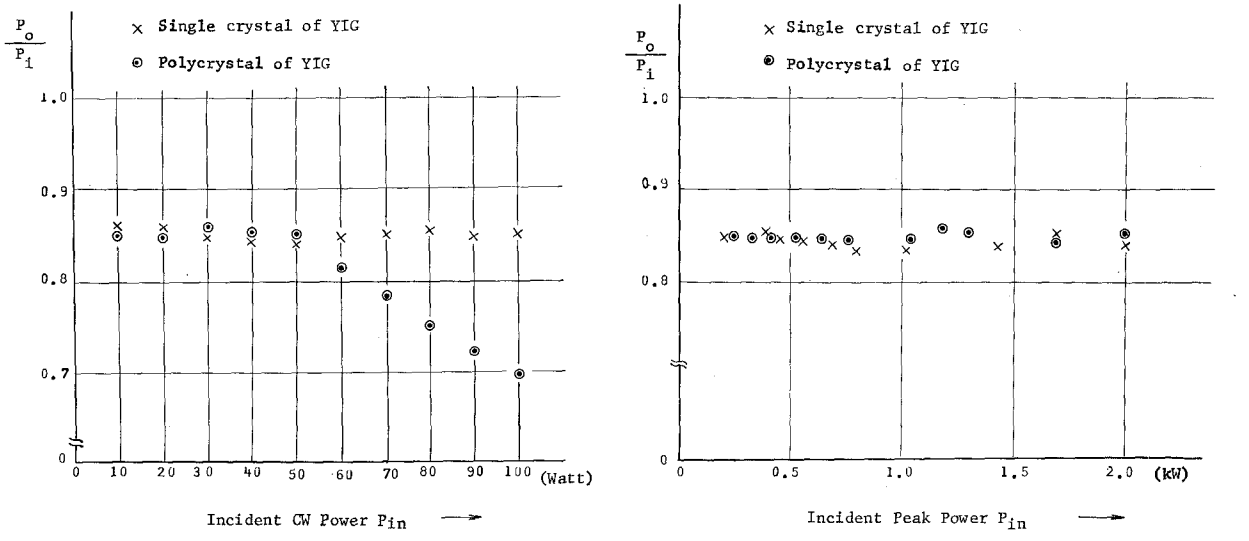

Fig. 4. Measured values of linearity of circulator with single crystal and polycrystal. P_0 is the output power from the circulator. (a) Linearity for CW power. (b) Linearity for pulsed power. Pulsewidth: 3 μs; repetition frequency: 300 Hz.

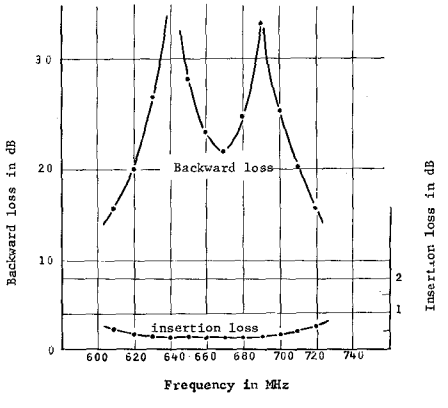

Fig. 5. Wideband characteristics of high-power UHF circulator.

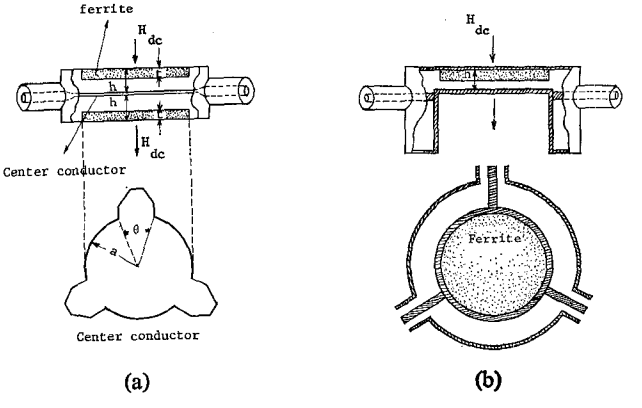

Fig. 6. Example of high-power circulator.

Substitute

$$y_2' = -\frac{Y}{\sqrt{3}}, \qquad y_3' = \frac{Y}{\sqrt{3}},$$
$$\alpha_i = 1 - |S_i| = \frac{3}{2}\frac{y_i''}{Y} \tag{47}$$

since

$$y_i = j\frac{2}{3}\omega(\tilde{W}_{e_i} - \tilde{W}_{m_i})$$
$$y_i'' = \frac{2}{3}\left(\frac{\omega\tilde{W}_{m_i}}{Q_i} + \frac{\omega\tilde{W}_{e_i}}{Q_c}\right) \fallingdotseq \frac{2}{3}\omega\tilde{W}_{m_i}\left(\frac{1}{Q_i} + \frac{2}{Q_c}\right). \tag{48}$$

Substituting (47) and (48) into (46)

$$L = 2.9\omega\tilde{W}_i k_f R\left(\frac{1}{Q_+} + \frac{1}{Q_-} + \frac{1}{Q_c}\right),$$
$$Q_2 = Q_-, \qquad Q_3 = Q_+. \tag{49}$$

Since the relation

$$\tilde{W}_i k_f = \frac{\sqrt{3}}{\tilde{\omega}R}\frac{\tilde{\mu}}{\mu_+ - \mu_-} = \frac{\sqrt{3}}{2\tilde{\omega}R}\frac{1}{\eta}$$

is derived from (4) and (6), substituting this relation into (49) under the approximation $\omega \fallingdotseq \tilde{\omega}$, we get

$$L = 2.51\frac{1}{\eta}\left(\frac{1}{Q_+} + \frac{1}{Q_-} + \frac{2}{Q_c}\right). \tag{50}$$

Appendix II

We have the field relation

$$\langle E_c J^* \rangle_{V+S} + \langle H_c M^* \rangle_{V+S} = 0 \tag{51}$$

where E_c and H_c are correct fields.[6] Maxwell's equations

$$\nabla \times H - j\omega\epsilon E = J, \qquad \nabla \times E + j\omega\mathfrak{u}H = -M \tag{52}$$

and boundary conditions

$$n \times [H_2 - H_1] = J, \qquad [E_2 - E_1] \times n = M \tag{53}$$

should be satisfied between trial field and current inside the medium with the tensor permeability $\mathfrak{u}$. If the same trial fields are used inside the medium with a scalar permeability μ, Maxwell's equations should be changed to

$$\nabla \times H - j\omega'\epsilon E = J',$$
$$\nabla \times E + j\omega'\mu H = -M' \qquad \omega' = \omega + \delta\omega \tag{54}$$

whereas boundary conditions are the same on discontinuous surfaces because of the same fields. Substituting the trial current obtained from (52) and (54) into (51),

$$\langle E_c \cdot \nabla \times H^* \rangle_V - \langle H_c \cdot \nabla \times E^* \rangle_V + j\omega\epsilon\langle E_c \cdot E^* \rangle_V + j\omega\langle H_c \cdot \mathfrak{u}^* H^* \rangle_V + \langle E_c J_S^* \rangle_S + \langle H_c M_S^* \rangle_S = 0 \tag{55}$$

$$\langle E_c \cdot \nabla \times H^* \rangle_V - \langle H_c \cdot \nabla \times E^* \rangle_V + j\omega'\epsilon\langle E_c E^* \rangle_V + j\omega'\langle H_c \cdot \mu^* H^* \rangle_V + \langle E_c J_S'^* \rangle_S + \langle H_c M_S'^* \rangle_S = 0. \tag{56}$$

Subtracting (55) from (56) and taking account of $J_S = J_S'$ and $M_S = M_S'$ because of the same boundary condition

$$\frac{\delta\omega}{\omega'} = \frac{-\langle H_c \cdot \mu^* H^* \rangle_V + \langle H_c \cdot \mathfrak{u}^* H^* \rangle_V}{\langle E_c \cdot \epsilon E^* \rangle_V + \langle H_c \cdot \mathfrak{u}^* H^* \rangle_V}$$

so that

$$\omega = \omega'\left\{1 - \frac{\iiint_\tau H \cdot (\mathfrak{u}^* - \mu) H^* dv}{2\iiint_V H \cdot \mathfrak{u}^* H^* dv}\right\}. \tag{57}$$

Acknowledgment

The author wishes to express his gratitude and appreciation to the Director of the Laboratories, Dr. M. Komai, for his encouragement and discussion in connection with this study. Thanks are also due to Mr. Hoshino for recording the experimental data.

References

[1] U. Milano, J. H. Saunders, and L. Davis, Jr., "A Y-junction strip-line circulator," *IRE Trans. Microwave Theory and Techniques*, vol. MTT-8, pp. 346–351, May 1960.

[2] H. Bosma, "On stripline Y-circulation at UHF," *IEEE Trans. Microwave Theory and Techniques*, vol. MTT-12, pp. 61–72, January 1964.

[3] C. V. Beuhler and A. F. Eikenberg, "A VHF high-power Y-circulator," *IRE Trans. Microwave Theory and Techniques (Correspondence)*, vol. MTT-9, pp. 569–570, November 1961.

[4] B. A. Auld, "The synthesis of symmetrical waveguide circulators," *IRE Trans. Microwave Theory and Techniques*, vol. MTT-7, pp. 238–246, April 1959.

[5] J. B. Davies and P. Cohen, "Theoretical design of symmetrical junction stripline circulators," *IEEE Trans. Microwave Theory and Techniques*, vol. MTT-11, pp. 506–512, November 1963.

[6] Y. Konishi, "VHF-UHF Y circulators," *Tech. J. Japan Broadcasting Corp.*, vol. 17, pp. 87–121, 1965. Also Nippon Hoso Kyokai, Tokyo, Japan, Tech. Monograph 6, May 1965.

[7] ——, "Lumped element Y circulator," *IEEE Trans. Microwave Theory and Techniques*, vol. MTT-13, pp. 852–864, November 1965.

[8] ——, "Characteristics of ferrite components and methods of approximate calculation for design," *Tech. J. Japan Broadcasting Corp.*, vol. 19, pp. 296–312, 1967.